

MECHANICAL SHOT NOISE INDUCED BY CREEP IN SUSPENSION DEVICES

May 22, 1997

**G. Cagnoli^(1,2), L. Gammaitoni^(1,2), J. Kovalik⁽¹⁾, F. Marchesoni^(1,3)
and M. Punturo⁽¹⁾**

(1) Istituto Nazionale di Fisica Nucleare, Sezione di Perugia, VIRGO Project,
I-06100 Perugia (Italy)

(2) Dipartimento di Fisica, Universita' di Perugia, I-06100 Perugia (Italy)

(3) Dipartimento di Fisica, Universita' di Camerino, I-62032 Camerino (Italy)

S. Braccini⁽⁴⁾, R. De Salvo⁽⁴⁾, F. Fidecaro^(4,5), A. Giazotto⁽⁴⁾, G. Losurdo^(4,6)

(4) Istituto Nazionale di Fisica Nucleare, Sezione di Pisa, VIRGO Project,
I-56010 S. Piero a Grado (Italy)

(5) Dipartimento di Fisica, Universita' di Pisa, I-56100 Pisa (Italy)

(6) Scuola Normale Superiore, I-56100 Pisa (Italy)

PACS 43.40.Cw, 62.40.+i, 05.40.+j

Abstract

The sensitivity curve of a gravitational wave interferometric detector like VIRGO might be seriously limited by the mechanical shot noise induced by stationary creep in the heavily loaded mechanical suspension components (wires, spring blades, etc.). We quantify this effect and discuss possible improvements which could be implemented without major design alterations.

1 INTRODUCTION

The interferometric detection of gravitational waves (GW) gained momentum over the last decade [1]-[3], as it became clear that low amplitude GW signals in the frequency range 1-50 Hz allow a significant GW source survey [4]. Two major such interferometers are presently under construction: LIGO [1] in the US and VIRGO [2] - [3] (a French-Italian collaboration) in Italy. Three main noise sources limit their sensitivity curve at low frequency: (i) the *seismic noise*,

due to ground vibrations, may be filtered through a network of cascaded linear mechanical filters; (ii) the *newtonian noise* (gravity gradient noise)[5], due to the local ground and atmospheric density fluctuations, is unavoidable in earth-based GW detectors; (iii) the *thermal noise*, mainly due to the internal friction [6]-[8] of the suspension (wires, springs, etc) and optical components (mirrors, beam-splitters, etc.), can be minimized by choosing appropriate materials, geometries and assembly procedures [9]-[15].

The design of the VIRGO suspensions involves a number of wires (see Fig. 1) and spring blades made of steel alloys (respectively, C85 steel and Maraging steel[17]) and subjected to a load of up to 65% of the relevant breaking point. Over the last four years of R&D activity, we addressed a simple question: how does the tensile stress exerted by the load affect the internal losses in a mechanical suspension? Preliminary results suggest that under realistic experimental circumstances, the loss angle $\phi(\omega)$ of a low frequency mechanical pendulum is (almost) independent of both the forcing frequency [9]-[13] and of the suspended load [9]-[11], [18].

The first property is reported (though not very well understood) in the earlier literature [6]-[8] and has been given a theoretical justification in recent years [13], [19]. The second property, instead, is likely due to the fact that $\phi(\omega)$ is determined experimentally over a relatively short time scale (the resonance period of the tested specimen), whereas on longer time scales (in a GW antenna data acquisition runs for years!) the creep phenomenon becomes detectable and might affect significantly the static relaxation properties of a mechanical device under tensile stress. As a result the mechanical losses consist of two independent contributions: the conventional internal friction (independent of load) and the mechanical shot noise related to the stationary creep mechanism (appreciable at high temperature and for heavy loads [8]). The latter source of noise belongs to the category of the so-called “excess noises” discussed in Ref. [20].

2 THE MODEL

We propose a simple model to determine the mechanical shot noise induced by the stationary creep in a loaded mechanical suspension. Following common understanding [8], we assume that the creep deformation results from single (quasi) instantaneous slippages occurring with size q_S and rate λ , both to be measured experimentally.

Let us look at the static length $l(t)$ of a loaded wire. Due to the creep mechanism (transient effects are ignored), l is modelled to grow with time according to the law

$$\tau_l \ddot{l} = -\dot{l} + \eta_S(t), \quad (1)$$

where $\beta = 1/\tau_l$ is a damping constant and $\eta_S(t)$ a shot noise source.

The constant β is the relaxation constant of the wire length after a slippage has occurred: the wire glitch takes place in a time interval not longer than l_0/c_l ,

where $c_l = \sqrt{E/\rho}$ is the longitudinal sound velocity in rods and l_0 is the wire rest length. Hence, on the average

$$\tau_l = l_0/2c_l. \quad (2)$$

Typically, for a metallic wire $\beta = 10^4 \text{ s}^{-1}$.

The shot noise $\eta_S(t)$ can be reproduced by a Poissonian sequence of equal pulses $h(t - t_i)$, each associated with a glitch of the wire. For simplicity, we assume that the Poisson rate is λ and that the η_S pulse at time t_i has the following shape

$$h(t - t_i) = \frac{q_S}{\tau_S} \exp[-(t - t_i)/\tau_S] \quad (t > t_i) \quad (3)$$

with integrated intensity q_S (glitch size). Moreover, we assume that $\tau_l \gg \tau_S$, namely the grain slippage duration τ_S is much shorter than the propagation time τ_l , so that $\lim_{\tau_S \rightarrow 0} h(t - t_i) = q_S \delta(t - t_i)$. Note that Eq. (1) can be easily integrated: due to a single pulse, l increases by

$$\Delta l = \int_{t_i}^{\infty} h(s - t_i) ds = q_S, \quad (4)$$

whence the step-wise growth of $l(t)$ assumed in the current literature [8].

Following [21], we derive immediately the power spectral density (p.s.d.) $S_S(\omega)$ of the stochastic force $\eta_S(t)$, namely

$$S_S(\omega) = 2\pi\delta(\omega) + \frac{q_S^2\lambda}{1 + (\omega\tau_S)^2}. \quad (5)$$

This means that $\langle \eta_S \rangle = q_S\lambda$ and $\sigma_S^2 = \langle (\eta_S - \langle \eta_S \rangle)^2 \rangle = q_S^2\lambda/2\tau_S$. The δ -like term of $S_S(\omega)$ corresponds to a linear increase $l_{dc}(t) = q_S\lambda t$ of the wire length $l(t)$, while the Lorentian curve on the r.h.s. of Eq. (5) characterizes its *zero-mean* noisy component $\delta_l(t)$.

3 MECHANICAL SHOT NOISE

The local control system of the VIRGO suspensions is designed to compensate the stationary creep in wires and spring blades [3]: this corresponds to subtracting the d.c. component of $l(t)$. Accordingly, in our model, we can set $\langle \eta_S \rangle = 0$ by construction and, correspondingly, ignore the δ -like term of $S_S(\omega)$ in Eq. (5).

The p.s.d. $S_\delta(\omega)$ of the subtracted wire length $\delta_l(t) = l(t) - l_{dc}(t)$ can be easily determined from Eq. (1), i.e.

$$S_\delta(\omega) = \frac{1}{1 + (\omega\tau_l)^2} \frac{S_S(\omega)}{\omega^2}. \quad (6)$$

At low frequencies. $\omega\tau_l \ll 1$ and $\omega\tau_s \ll 1$,

$$S_\delta(\omega) \simeq q_S^2 \frac{\lambda}{\omega^2}. \quad (7)$$

The vertical displacement $z(t)$ of a pointlike mass suspended by an *elastic* wire with constant static length [during data acquisition, $l_{dc}(t)$ is locked to a given reference value], is governed by the full stochastic differential equation

$$\ddot{z} = -\gamma\dot{z} - \omega_0^2 z + \omega_0^2 \delta_l(t), \quad (8)$$

where $\nu_0 = \omega_0/2\pi$ is the resonance frequency of the vertical mode and $\gamma = \gamma(\omega)$ is the damping constant due to the internal friction, $\gamma(\omega) \propto \phi(\omega)/\omega$.

The p.s.d. for the variable $z(t)$ follows immediately

$$S_z(\omega) = |\chi(\omega)|^2 S_\delta(\omega), \quad (9)$$

where

$$\chi(\omega) = \omega_0^2 / [(\omega_0^2 - \omega^2) + i\gamma\omega]. \quad (10)$$

The corresponding vertical fluctuation amplitude $|z(\omega)|$ reads:

$$|z(\omega)| \simeq \frac{\omega_0^2}{\sqrt{(\omega^2 - \omega_0^2)^2 + \gamma^2\omega^2}} \frac{q_S \sqrt{\lambda}}{\omega}, \quad (11)$$

or, for $\nu_0 \ll \nu \ll \tau_l^{-1}, \tau_s^{-1}$,

$$|z(\nu)| \simeq \left(\frac{\nu_0}{\nu}\right)^2 \frac{q_S \sqrt{\lambda}}{2\pi\nu}. \quad (12)$$

The unreduceable vertical-horizontal coupling factor, due to the earth curvature over the distance between two VIRGO mirrors. $L = 3$ km, is of the order of $\theta = 3 \cdot 10^{-4}$ rad (a larger coupling factor ($10^{-2} - 10^{-3}$) could come from the mechanical imperfections on the suspension chain) whence the horizontal fluctuation amplitude of each suspended mass:

$$|x(\nu)| = \theta |z(\nu)| \quad (13)$$

By summing up *in quadrature* (whence the multiplicative factor $\kappa_C = 2$) the fluctuations induced by the mechanical shot noise on each mirror of the interferometer and introducing the geometric factor $\kappa_m \geq 2$ which accounts for the suspension wire loops of Fig. 1, we eventually estimate the relevant contribution to the VIRGO sensitivity curve [2], [3], namely

$$\bar{h}_C(\nu) = \theta \frac{\kappa_C}{\kappa_m} \left(\frac{\nu_0}{\nu}\right)^2 \frac{q_S}{L} \frac{\sqrt{\lambda}}{2\pi\nu}. \quad (14)$$

An upper-bound curve for $\bar{h}_C(\nu)$ is plotted in Fig. 2.

4 ESTIMATE OF THE GLITCH SIZE

In the absence of conclusive experimental data, we have recourse to a qualitative argument to set an *upper bound* to q_S . Let us consider a polycrystalline specimen of C85 steel (the material chosen for VIRGO suspension wires): the average grain radius r_g ranges between 2 and $5\mu\text{m}$, to compare with the radius $r_w=100\mu\text{m}$ of the wire cross-section. Typical values for the grain boundary slippage δr_g , reported in the metallurgy handbooks, are 40 – 100nm. On a microscopic scale, a grain slippage occurs when the applied stress builds up locally above a certain threshold of the order of the wire breaking stress σ_b . The ensuing elastic energy release, $(\pi/2)(\sigma_b r_g^2)\delta r_g$, generates an acoustic wave burst and, eventually, thermal dissipation. Accordingly, on a macroscopic scale the potential energy of the suspended mass M must decrease by the same amount. Since each VIRGO wire is loaded approximately up to half its breaking point, that is $Mg = (\pi/2)\sigma_b r_w^2$, the energy balance requires that

$$\frac{\pi}{2}(\sigma_b r_g^2)\delta r_g = \frac{\pi}{2}(\sigma_b r_w^2)q_S, \quad (15)$$

whence

$$q_S = \delta r_g (r_g/r_w)^2. \quad (16)$$

On inserting the estimated values for r_g and δr_g available in the literature, we conclude that $q_S \simeq 10^{-10}\text{m}$. Note that Eq. (16) overestimates q_S on several accounts: grain slippages are mostly rotational, whereas in Eq. (15) δr_g is treated like a grain translation; the dissipation of the released elastic energy is assumed to occur on one very short time scale τ_S , with $\tau_S \ll \tau_l$, whereas it might involve also time scales substantially longer than τ_l . Most importantly, we neglected the dislocation movements inside individual grains. That would yield a much smaller slip unit (of the order of the relevant Burger's vector $b \sim 3 \cdot 10^{-10}\text{m}$), which is generally assumed [8] to be responsible for the transient creep laws at low stresses. *Annealing* is expected to quench the latest source of "excess noise" [3].

5 CREEP MEASUREMENTS

The experimental determination of the glitch size q_S and the glitch rate λ for a given specimen is a rather delicate matter. The only observable we succeeded in investigating experimentally (under the VIRGO operating conditions) so far, is the creep rate μ , defined as [8]

$$\delta l = \mu \delta t, \quad (17)$$

where δl is the wire length increment caused by stationary creep (that is, after subtracting elastic elongation) in the time interval δt . On assuming that all

Table 1: Technical parameters for the Virgo mirror suspension wires

	length (<i>cm</i>)	diameter (μm)	material	breaking load (<i>N</i>)	working load (<i>N</i>)	Therm. exp. coeff. (K^{-1})
far mirror wire	70	300	C85	187	105	$14.9 \cdot 10^{-6}$
near mirror wire	70	200	C85	89	53	$14.9 \cdot 10^{-6}$

glitches are equal size, we can easily combine the glitch parameters to obtain

$$\mu = q_s \lambda. \quad (18)$$

The experimental set-up developed in Perugia to measure the creep rate in the suspension wires of the VIRGO mirrors is sketched in Fig. 3 (a similar set up devoted to the measurement of creep rates in suspension blades and in the filter suspension wires, has been developed in Pisa [17]). Samples of the VIRGO wires (see Table I) were loaded up to 5 kg in vacuum.

Each test wire was suspended from an INVAR steel column (with cross section of 5 cm and thermal expansion coefficient of $0.91 \cdot 10^{-6} K^{-1}$) by means of a standard VIRGO clamp [3] - a specially designed vise where the top of the wire is squeezed between two plates of HS steel. The load was attached to the wire by means of a similar clamp, with the steel plates replaced by brass plates.

The wire elongation was measured by determining the position of the suspended mass with respect to the pedestal of the INVAR column. Such a procedure is affected by systematic errors, due to thermal effects on the column length, the position read-out device and the wire itself. For this reason, the vacuum chamber was equipped with an automatic thermostatzation system (stability 0.01K); the residual (local) thermal fluctuations were recorded during each data acquisition and the relative thermal expansions of the column and the wire eventually subtracted. The thermal expansion coefficients of both the column and the wire were measured directly in situ. The position read-out device was a shadow-meter with an accuracy of $0.1 \mu m$ per 3 days of data acquisition; its geometry and dimensions were configured in order to minimize the effects of the possible thermal expansions of its components. A thermostatzation system maintained the temperature of the test wire at 150 C. This is the temperature forseen for the vacuum bake out (one week) of the assembled mechanical suspensions of the VIRGO antenna [3].

We measured the creep in loaded C85 steel wires (see Table I) at three different points of the baking cycle: (a) at $T = 35$ C, before baking; (b) at $T = 150$ C, during baking; (c) at $T = 27$ C, after baking. Our results are shown

in Figs. 4-6, respectively. Figs. 4 and 5 display the typical logarithmic law for the creep phenomenon at low temperatures [22][23]. On fitting the data in Figs. 4 and 6, we extracted our experimental estimates for the creep rates μ_{bb} and μ_{ab} , before and after baking, respectively, that is:

$$\mu_{bb}(t) = \frac{\mu_0}{1 + t/t_0}, \quad (19)$$

where $\mu_0 = 1.4 \cdot 10^{-8} \text{ m s}^{-1}$ and $t_0 = 1.85 \cdot 10^5 \text{ s}$, and

$$\mu_{ab} = 2 \cdot 10^{-14} \text{ ms}^{-1}. \quad (20)$$

One sees immediately that in C85 wire samples prior to the baking cycle the creep rate is dominated by transient (or non-stationary) relaxation mechanisms, mainly due to dislocation depinning from point defects inside the crystal grains. After heating for one week at 150 C, the dislocation dynamics comes to a halt and grain-boundary slippages seem to produce the largest contribution. Note that according to the fitting law (19), after a one-year run, μ_{bb} would be still three orders of magnitude larger than μ_{ab} . Thus, baking is the best solution so far for reducing the creep disturbances in the mirror suspensions.

6 CONCLUSIONS

We conclude by drawing an upper-bound to the shot noise contribution $\tilde{h}_C(\nu)$ to the VIRGO sensitivity curve - see Fig. 2. The quantities q_S and λ enter our prediction (14) for $\tilde{h}_C(\nu)$ and (18) for μ in different ways, so that, in principle, one should determine such quantities separately, by measuring two independent macroscopic observables. Improved acoustic emission together with interferometric techniques might prove adequate to characterize the glitch rate and also the glitch size distribution directly.

Here, we limit ourselves to noticing that our estimate (16) sets an upper bound to q_S . The mechanical shot noise term $\tilde{h}_C(\nu)$, Eq. (14), is thus proportional to $\sqrt{q_S \mu}$, where for μ one must take μ_{ab} in Eq. (20). The ensuing curve for $\tilde{h}_C(\nu)$ with $q_S = 10^{-10} \text{ m}$ is plotted in Fig. 2: the mechanical shot noise contributes to the overall VIRGO sensitivity curve, between 10 Hz and 50 Hz a small fraction of the thermal noise.

Moreover, should the estimated low glitch rate (only a few glitches per hour) be confirmed by a direct measurement, the oscillation bursts of the detector control signals caused by the suspension creep might be subtracted altogether. Isolated bursts could be identified and discarded, even during the antenna data acquisition (i.e. in real time) [3], provided that the glitch shape and size distribution are known.

Experimental tests to measure the glitch rate and shape in wires (C85 steel which is the VIRGO reference solution for test mass suspension wires, but also in other promising materials, like Maraging) are in progress.

References

- [1] A. Abramovici *et al*, *Science* **256** 325 (1992)
- [2] A. Giazotto, *Phys. Rep.* **C182** 365 (1989); C. Bradaschia *et al*, *Nuc. Instr. Meth. Phys. Res.* **A289** 518 (1990)
- [3] VIRGO Collaboration, *The VIRGO Final Conceptual Design*, unpublished (1995)
- [4] K. S. Thorne, *300 Years of Gravitation* (CUP, Cambridge, 1987)
- [5] P. R. Saulson, *Phys. Rev.* **D30** 732 (1984)
- [6] A. S. Nowick and B. S. Berry, *Anelastic Relaxation in Crystalline Solids* (Academic, New York, 1972)
- [7] A. V. Granato and K. Lücke, in *Physical Acoustics*, eds. W. P. Mason and R. N. Thurston (Academic, New York, 1966), Vol IVA, p. 225
- [8] F. R. N. Nabarro, *Theory of Crystal Dislocations* (Oxford University Press, London, 1967)
- [9] T. J. Quinn, C. C. Speake, W. Tew, R. S. Davis and L. M. Brown, *Phys. Lett.* **A197** 197 (1995)
- [10] G. Cagnoli, L. Gammaitoni, J. Kovalik, F. Marchesoni and M. Punturo, *Phys. Lett.* **A213** 245 (1996)
- [11] T. J. Quinn, C. C. Speake and L. M. Brown, *Phil. Mag.* **A65** 261 (1991)
- [12] P. R. Saulson, *Phys. Rev.* **D42** 2437 (1990); P. R. Saulson, R. T. Stebbins, F. D. Dumont and S. E. Mock, *Rev. Sci. Instrum.* **65** 182 (1994)
- [13] G. Cagnoli, L. Gammaitoni, F. Marchesoni and D. Segoloni, *Phil. Mag.* **68** 865 (1993)
- [14] A. Gillespie and F. Raab, *Phys. Lett.* **A178** 357 (1993), **A190** 213 (1994)
- [15] J. E. Logan, J. Hough and N. A. Robertson, *Phys. Lett.* **A183** 145 (1993)
- [16] F. Bondu, Jean-Yves Vinet, *Physics Letters A* 198 (1995) 74
- [17] S. Braccini *et al.*, 1997 (to be published)
- [18] Y. Huang and P. R. Saulson, *Rev. Sci. Instrum.* **65** 2102 (1994)
- [19] F. Marchesoni and M. Patriarca, *Phys. Rev. Lett.*, **72** 4101 (1994)

- [20] A. Yu. Ageev, I. A. Bilenko, V. B. Braginsky and S. P. Vyatchanin, *Phys. Lett.* **A227** 159 (1997)
- [21] A. Papoulis, *Probability, Random Variables and Stochastic Processes* (Mc Graw-Hill, New York, 1991)
- [22] A. H. Cottrell, *J. of Mech. Phys. Solids* **1** 53-63 (1952)
- [23] A. Oehlert and A. Atrens, *Acta metall. mater.* **42** (5) 1493-1508 (1994)

Figure 1: Sketch of the last suspension stage of the VIRGO interferometer.

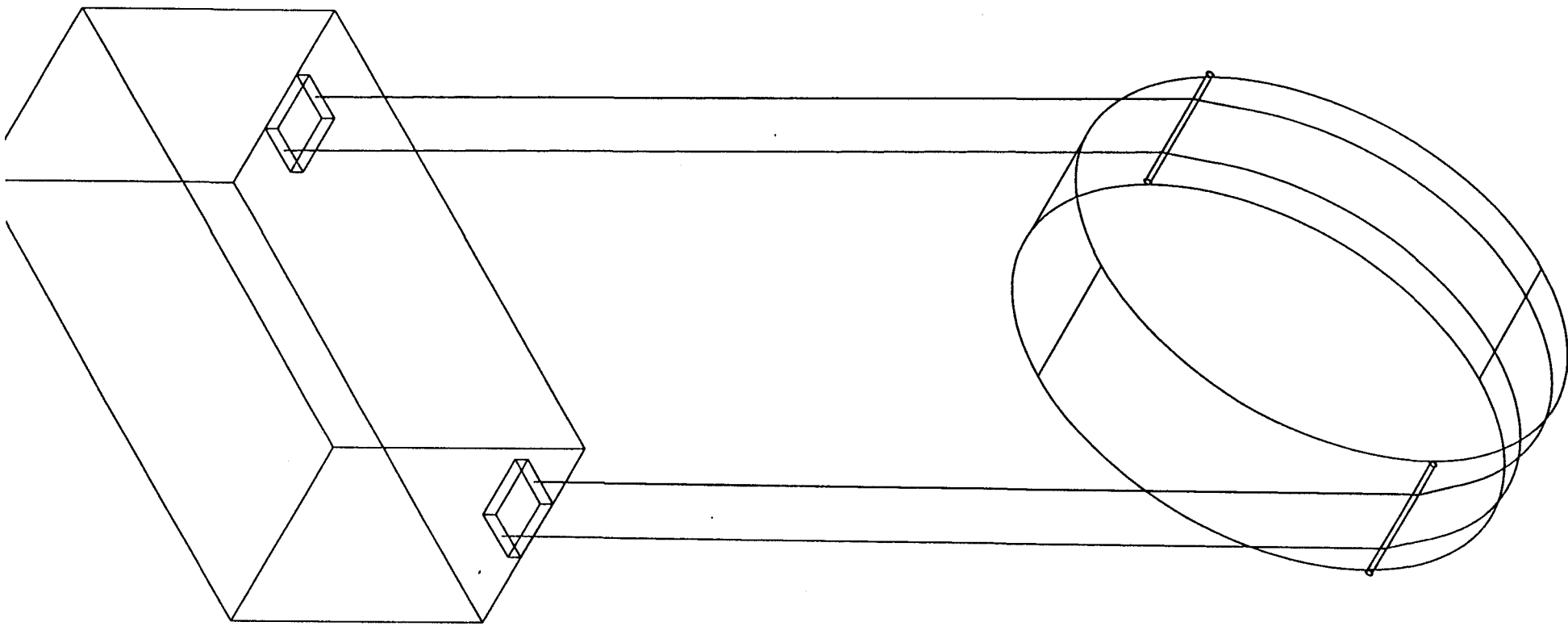
Figure 2: The VIRGO sensitivity curve. Pointed lines represent the estimated contributions from different noise sources. The solid thick line is the resulting sensitivity curve. Our upper bound 14 (with $\mu_{ab} = 2 \cdot 10^{-14} \text{ms}^{-1}$ and $q_S = 10^{-10} \text{m}$, $\theta = 3 \cdot 10^{-4} \text{rad}$) for the mechanical shot noise contribution is represented by a thin solid line.

Figure 3: Experimental setup employed to measure the suspension wire stretching.

Figure 4: Wire stretching before baking. Solid line: elongation in 10^{-6}m , left axis. Squares: wire temperature, right axis. Dashed line: logarithmic fit $\Delta L = 51.2 \ln(1 + (t/51.3h))10^{-6} \text{m}$.

Figure 5: Wire stretching at 150 degrees. Dotted line: temperature, right axis. Dashed line: wire stretching (thermal expansion + creep effect), left axis. Solid line: wire stretching after subtracting the thermal expansion, left axis.

Figure 6: Wire stretching after baking. The wire employed in fig. 3 has been tested for residual stretching at $T = 27 \text{ C}$. Dots: elongation in 10^{-9}m . Solid line: linear fit $\Delta L = \mu_{ab}t$ with $\mu_{ab} = (2 \pm 1)10^{-14} \text{m/s}$.



Virgo Sensitivity Curve

